Nuclear Instruments and Methods in Physics Research B 352 (2015) 202–205

Contents lists available at ScienceDirect

Nuclear Instruments and Methods in Physics Research B

journal homepage: www.elsevier.com/locate/nimb

Computer simulations of material ejection during C_{60} and Ar_m bombardment of octane and β-carotene

G. Palka [a], M. Kanski [a], D. Maciazek [a], B.J. Garrison [b], Z. Postawa [a,*]

[a] Smoluchowski Institute of Physics, Jagiellonian University, ul. Reymonta 4, 30-059 Krakow, Poland
[b] Department of Chemistry, 104 Chemistry Building, Penn State University, University Park, PA 16802, USA

ARTICLE INFO

Article history:
Received 11 July 2014
Received in revised form 9 October 2014
Accepted 29 November 2014
Available online 30 December 2014

Keywords:
Molecular dynamics simulations
SIMS
Cluster bombardment

ABSTRACT

Molecular dynamics (MD) computer simulations are used to investigate material ejection and fragment formation during keV C_{60} and Ar_m (m = 60, 101, 205, 366, 872 and 2953) bombardment of organic solids composed from octane and β-carotene molecules at 0° and 45° impact angle. Both systems are found to sputter efficiently. For the octane system, material removal occurs predominantly by ejection of intact molecules, while fragment emission is a significant ejection channel for β-carotene. A difference in the molecular dimensions is proposed to explain this observation. It has been shown that the dependence of the sputtering yield Y on the primary kinetic energy E and the cluster size n can be expressed in a simplified form if represented in reduced units. A linear and nonlinear dependence of the Y/n on the E/n are identified and the position of the transition point from the linear to nonlinear regions depends on the size of the cluster projectile. The impact angle has a minor influence on the shape of the simplified representation.

1. Introduction

Molecular dynamics (MD) computer simulations are an excellent tool for acquiring a better understanding of the processes that occur during cluster bombardment of solids [1]. Through the use of computer modeling, a microscopic view of how projectiles interact with the substrate can be captured [1,2]. Computational research of the processes induced by cluster projectiles has drawn much attention since it was found that such projectiles allow depth profiling of certain organic materials by secondary ion mass spectrometry (SIMS) [3]. As a result, study of material emission and damage formation caused by a cluster bombardment is currently one of the most interesting research endeavors. Both experimental and theoretical studies indicate that the sputtering efficiency depends on projectile and target parameters [1,2]. It has been also shown that this dependence can be greatly simplified if a special representation is adopted [4–6]. In this, so-called "universal" representation the total ejected mass Y_{mass} or the sputtered volume Y_v is divided by the number of nucleons in the projectile n (or the total number of projectile atoms if projectiles are homogenous) and plotted as a function of the total kinetic energy of the cluster projectile E divided by the number of nucleons. The existence of two regions of sputtering is observed in such plot depending on the E/n [4–6]. At high E/n all data points can be plotted on a single line and dependence between Y/n and E/n is approximately linear. In other words, the sputtering yield is proportional to the total projectile kinetic energy. At lower E/n the dependence between Y/n and E/n becomes nonlinear and the sputtering yield depends on projectile nuclearity.

Unfortunately, the Y/n vs E/n plots published in the literature contain the data for a limited number of projectile kinetic energies and projectile sizes. As a result, the data points are scattered at least in the low E/n energy region. There is usually also a gap in the middle of the transition region. The goal of this study is to investigate systematically the effect of the size and the kinetic energy of the cluster projectile on the ejection efficiency of intact molecules and fragments from two different organic solids. Samples composed from small (octane – C_8H_{18} – length ~0.9 nm) and medium (β-carotene – $C_{40}H_{56}$ – length ~2.9 nm) sized molecules were selected to probe the effect of molecular dimension on the ejection characteristics. The organic samples were bombarded by keV C_{60} and Ar_m (m = 60, 101, 205, 366, 872 and 2953) projectiles at 0° and 45° within a range of kinetic energies to reproduce conditions usually applied in experiments.

2. Simulation and model

Detailed description of molecular dynamics computer simulations used to model cluster bombardment can be found elsewhere

* Corresponding author. Tel.: +48 (12) 664-4626.
E-mail address: zbigniew.postawa@uj.edu.pl (Z. Postawa).

http://dx.doi.org/10.1016/j.nimb.2014.11.108
0168-583X/

[1]. Briefly, the motion of the particles is determined by integrating Hamilton's equations of motion. The forces among the particles are described by a blend of pair-wise additive and many-body potential energy functions. The atomistic AIREBO potential is used to describe interactions among hydrocarbon atoms [7]. This potential describes respectably well reactions among these species, in particular, dissociation and *H* addition and abstraction [8]. The interactions between Ar atoms in the projectile and between the projectile atoms and all other particles in the system are described by the Lennard-Jones potential splined with the KrC potential to properly describe high-energy collisions [9]. Of note is that octane is a saturated hydrocarbon molecule with no readily available opportunity for crosslinking, while β-carotene has double bonds which can cross-link. The original organic systems had geometrical configurations and densities equal to the values measured in experiments at room temperature, i.e. 0.70 g/cm^3 and 0.94 g/cm^3. Samples were subsequently equilibrated to achieve the most optimal configurations for the potentials used. The calculated density of equilibrated octane and β-carotene samples is 0.87 g/cm^3 and 0.97 g/cm^3, respectively. The larger density can be attributed to the lower sample temperature in our calculations and to the imperfections of the AIREBO potential.

The calculated surface binding energy of molecules is approximately 0.5 eV and 1.5 eV for octane and β-carotene, respectively. The approximate diameter of the hemispherical sample cut-out after equilibration procedure is 38 nm. The model systems contain 57,452 and 14,620 octane and β-carotene molecules, respectively. Rigid and stochastic regions with a thickness of 0.7 and 2.0 nm, respectively, were used around the hemisphere to preserve the shape of the sample and to simulate the thermal bath that keeps the sample at the required temperature and helps inhibit the pressure wave reflection from the system boundaries [10]. The cluster projectiles were used to bombard the crystal with the kinetic energy ranging between 0.4 and 30 keV and an impact angle of 0° and 45°. Such values were selected to reproduce conditions used in the experimental studies. As it has been shown, the efficiency of a cluster sputtering process of organic materials weakly depends on the projectile impact point. Consequently, only two impacts were probed [11]. The simulations were run at 0 K target temperature and extend up to 50 ps which is long enough to see a saturation in the sputtering yield vs time dependence.

3. Results

The calculated total sputtering yields, expressed in number of ejected molecules, induced by keV C_{60} and Ar_{872} bombardment at 45° incidence are shown in Fig. 1 for octane and β-carotene, respectively. There are several interesting observations that can be made from the data presented in this figure. For both materials the sputtering yield is significant which can be attributed to a low cohesive energy of both solids. The yield increases linearly with the impact kinetic energy above a certain energy. The slope of the straight line increases with the cluster size. The linear dependence of the sputtering yield on the kinetic energy of a cluster projectile has been observed previously and is attributed to a deposition of a projectile kinetic energy in the subsurface volume from where ejection occurs [2,4,12]. At the same sputtering conditions, the total sputtering yield is much larger for octane than for β-carotene which could be attributed to a lower binding energy of the former solid and to a smaller size of octane molecules. The total mass of ejected material is, however, comparable as the β-carotene molecule is almost 5 times more massive than octane. Interestingly, for impact angles close to 45° the total yields for C_{60} and Ar_{872} are quite similar for a given molecule and energy. We attribute this fact to the enhanced molecular ejection caused by the washing-off mechanism observed for large cluster projectiles [13]. The fragmentation process is more pronounced for β-carotene and for C_{60} projectiles. As shown in Fig. 2, the total emission of organic material first increases with the projectile size as the primary kinetic energy is deposited closer to the surface [14], and subsequently decreases as the cluster projectile becomes large due to a decreased density of deposited energy [14] and a blocking of ejecting molecules in the direction close to the surface normal by a cloud of hovering projectile atoms. This phenomenon leads to a so called lateral sputtering [15]. The number of molecular fragments monotonically

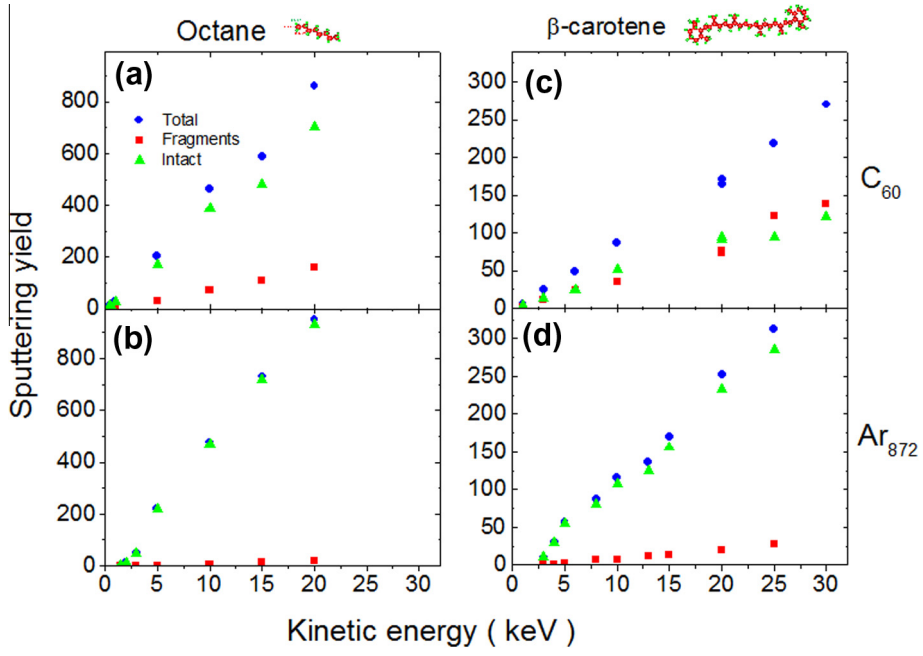

Fig. 1. The calculated total sputtering yields, expressed in number of ejected molecules, induced by (a) and (c) keV C_{60} and (b) and (d) Ar_{872} bombardment of (a) and (b) octane and (c) and (d) β-carotene at 45°. The total sputtering yield and the sputtering yield of fragments and intact molecules is represented by blue circles, red squares and the green triangles, respectively. (For interpretation of the references to colour in this figure legend, the reader is referred to the web version of this article.)

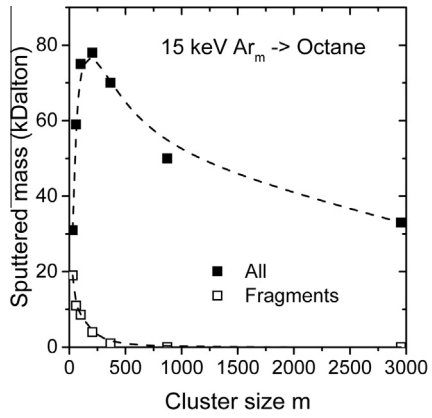

Fig. 2. Dependence of the sputtering yield of all particles (squares) and fragments (empty squares) expressed in mass units on the cluster size m of Ar_m projectiles bombarding octane sample at 45° impact angle. Broken lines are shown to guide the eye.

decreases with an increase of the projectile size for a given kinetic energy. This is caused by a decreasing kinetic energy carried out by an individual projectile atom which results in more gentle collisions and, consequently, a lower fragmentation.

Fragmentation occurs very fast and within 2 ps almost 91% of fragments recorded at 50 ps are created in both solids. The fragments are created predominantly by direct interactions with projectile atoms. It should be pointed out, however, that additional fragmentation will occur at μs timescales of experiments, for instance, by unimolecular decay of internally excited molecules [5]. As shown for PS oligomers, while this process has significant impact on ejection of slow molecules, its contribution to the total number of created fragments is less crucial than the contribution of collisional fragmentation [5]. Molecular fragments are formed in the energized volume located close to the projectile point of impact [5,16]. This zone is surrounded by the volume from where the intact molecules are emitted by a hydrodynamic-like flow (faster molecules that are emitted soon after the projectile impact) and effusive-like emission that leads to ejection of slow molecules [17]. As already mentioned, molecular ejection is hindered when bombarded with large projectiles. In this case, a cloud of hovering projectile atoms is formed which blocks ejection of material in the direction close to the surface normal. We see that the effect of this process decreases with the increase of the kinetic energy, because the hovering cloud is dispersed sooner.

The fraction of sputtered molecules that are ejected as fragments is much greater from β-carotene than from octane. Inspection of computer animations shows that a difference in the molecular size is mainly responsible for this difference. Octane molecules are small, approximately 0.9 nm long. It is relatively easy, therefore, to uplift these particles without fragmentation. On the other hand, β-carotene molecules are more than 3 times longer (~2.9 nm) and contain almost 4 times as many atoms. Ejection of the larger molecules requires a concerted action of many surrounding particles [18]. The probability of such correlated action decreases rapidly with the number of particles involved. As a consequence, ejection of intact molecules from β-carotene system will be more difficult than from octane. Moreover, it is also much easier to destroy a large molecule as various uncorrelated forces may act on different parts of this structure. Both these processes will result in a lower emission of intact molecules, and a higher ejection of molecular fragments from β-carotene as compared to octane, which is indeed observed.

The data presented in Fig. 1 show that the sputtering efficiency depends on both the kinetic energy and the size of the projectile cluster. It has been shown that the relation between the sputtering efficiency and parameters of the cluster projectiles can be significantly simplified if the data are presented in a special form [4,5]. Such representation, sometime called "universal", is shown in Fig. 3 for octane and β-carotene. Indeed, at the high E/n region all data points are located at the same line and the dependence between Y_{mass}/n and E/n is linear, where Y_{mass} is the total mass of ejected material. This observation is not true for fragment emission which is always larger for β-carotene than for octane. There is a strong decrease of fragment formation for $E/n = 1$ eV. As a result, in this energy regime only intact molecules are ejected which offers new analytical perspectives for SIMS. At low E/n value, the data points cannot be placed on a single line and the Y_{mass}/n vs E/n dependence becomes nonlinear as reported previously [5]. We observe, however, that the onset of the nonlinear region depends strongly on the cluster size, shifting it to the lower kinetic energy per nucleon as the size of the cluster projectile increases. This is a new observation that could not be done from previously published plots for organics due to a large spread of the calculated data. This is an important observation as it has been proposed previously that the transfer from the linear to nonlinear region occurs when the rate of the energy deposition becomes comparable with the rate this energy can be drained away from the sputtering region into the sample. As a consequence of such energy depletion, less energy is available for sputtering and the yield decreases faster than E/n. The energy deposition rate depends on the velocity of the cluster projectile, which, in turn, depends on the size of the projectile for a given kinetic energy E. On the other hand, the energy depletion rate should depend only on the material properties of the bombarded solid. All data points in Fig. 3 corresponding to the same kinetic energy per nucleon have the same velocity. As a result, one would expect that the transition from the linear to nonlinear region should occur at the same E/n. In other words, it should not depend on the cluster size. This is evidently not happening which indicates that some additional processes should be taken into account. The nature of these processes is unknown at the moment. An abrupt decay of the sputtering yield below certain E/n may be associated, for instance, with a blocking effect of hovering projectile atoms. We are currently investigating this phenomenon.

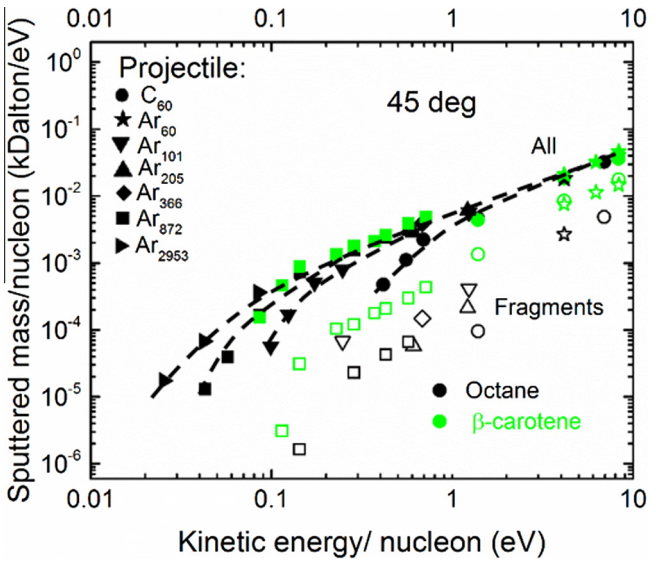

Fig. 3. Dependence of the total ejected mass Y_{mass} per projectile nucleon on the projectile kinetic energy per nucleon for the total mass (full symbols) and the mass of fragments (open symbols) ejected from octane (black) and β-carotene (green) at 45° impact angle. Broken lines are shown to guide the eye. (For interpretation of the references to colour in this figure legend, the reader is referred to the web version of this article.)

The impact angle has a minor influence on the shape of Y/n vs E/n plot. It is known that the sputtering yield induced by medium size projectiles like C_{60} or Ar_{60}, initially does not change much with the increase of the impact angle and then decreases [13]. A different behavior was reported for large cluster projectiles, where the sputtering yield may initially increase significantly with the impact angle [13]. However, the changes of the sputtering yields for impact angles 0° and 45° are relatively small for projectiles smaller than Ar_{366}. Only for larger projectiles the yield significantly increases at 45° as compared to the normal incidence, and the data points for these clusters (Ar_{872} and Ar_{2953}) in Fig. 3 are placed noticeably lower for normal incidence.

4. Conclusions

Molecular dynamics simulations have been performed to model bombardment of organic solids of octane and β-carotene by keV C_{60} and Ar_m projectiles. Because of the relatively small cohesive energy compared with, for example, metals, the total sputtering yield for both these solids is high. For octane, of the total sputtering yield, approximately 85% is in intact molecules and the remainder in fragments. For β-carotene the situation is different and much more material is emitted as fragments. A difference in the molecular size is responsible for such behavior. The dependence of the total sputtered mass Y_{mass} on the primary kinetic energy E and the cluster size n can be expressed in a simplified form if represented in reduced units of Y_{mass}/n and E/n, where n is the number of nucleons in the projectile. It is shown that the position of the transition point from the linear and nonlinear region of the $Y_{mass}/n(E/n)$ dependency shifts to lower E/n as the size of the cluster projectile increases. This observation rather disqualifies the interplay between the rate of deposited energy and the rate of energy transfer from the sputtering region into the sample as the sole explanation for existence of the nonlinear region. The impact angle has a minor influence on the shape of the Y_{mass}/n vs E/n, except for the data points corresponding to Ar_{872} and Ar_{2953} projectiles.

Acknowledgments

The authors gratefully acknowledge financial support from the Polish National Science Center, Program Nos. 2013/09/B/ST4/00094. We appreciate the support of the Penn State Research Computing and Cyberinfrastructure group in performing these simulations.

References

[1] B.J. Garrison, Z. Postawa, Mass Spectrom. Rev. 27 (2008) 289–315.
[2] B.J. Garrison, Z. Postawa, in: J.C. Vickerman, D. Briggs (Eds.), ToF-SIMS – Surface Analysis by Mass Spectrometry, second ed., IMP & SurfaceSpectra Ltd., Chichester & Manchester, 2013, pp. 151–192.
[3] N. Winograd, Anal. Chem. 77 (2005) 142A–149A.
[4] C. Anders, H.M. Urbassek, R.E. Johnson, Phys. Rev. B 70 (155404) (2004) 155401–155406.
[5] A. Delcorte, B.J. Garrison, K. Hamraoui, Anal. Chem. 81 (2009) 6676–6686.
[6] M.P. Seah, J. Phys. Chem. C 117 (2013) 12622–12632.
[7] S.J. Stuart, A.B. Tutein, J.A. Harrison, J. Chem. Phys. 112 (2000) 6472–6486.
[8] B.J. Garrison, P.B.S. Kodali, D. Srivastava, Chem. Rev. 96 (1996) 1327–1341.
[9] R.A. Aziz, M.J. Slaman, Mol. Phys. 58 (1986) 679–697.
[10] Z. Postawa, B. Czerwinski, M. Szewczyk, E.J. Smiley, N. Winograd, B.J. Garrison, Anal. Chem. 75 (2003) 4402–4407.
[11] B. Czerwinski, R. Samson, B.J. Garrison, N. Winograd, Z. Postawa, Vacuum 81 (2006) 167–173.
[12] M.F. Russo, K.E. Ryan, B. Czerwinski, E.J. Smiley, Z. Postawa, B.J. Garrison, Appl. Surf. Sci. 255 (2008) 897–900.
[13] B. Czerwinski, L. Rzeznik, R. Paruch, B.J. Garrison, Z. Postawa, Nucl. Instr. Meth. Phys. Res. B Beam Interact. Mater. Atoms 269 (2011) 1578–1581.
[14] E.J. Smiley, N. Winograd, B.J. Garrison, Anal. Chem. 79 (2007) 494–499.
[15] Z. Insepov, I. Yamada, M. Sosnowski, Mater. Chem. Phys. 54 (1998) 234–237.
[16] B.J. Garrison, Z. Postawa, K.E. Ryan, J.C. Vickerman, R.P. Webb, N. Winograd, Anal. Chem. 81 (2009) 2260–2267.
[17] D.A. Brenes, Z. Postawa, A. Wucher, P. Blenkinsopp, B.J. Garrison, N. Winograd, J. Phys. Chem. Lett. 2 (2011) 2009–2014.
[18] B.J. Garrison, A. Delcorte, K.D. Krantzman, Acc. Chem. Res. 33 (2000) 69–77.